Chemical Engineering Journal 218 (2013) 267–275

Contents lists available at SciVerse ScienceDirect

Chemical Engineering Journal

journal homepage: www.elsevier.com/locate/cej

A hypercrosslinked poly(styrene-co-divinylbenzene) PS resin as a specific polymeric adsorbent for adsorption of 2-naphthol from aqueous solutions

Jianhan Huang [a,b,c,*], Xiaofei Wu [b], Hongwei Zha [a], Bin Yuan [b], Shuguang Deng [b,*]

[a] School of Chemistry and Chemical Engineering, Central South University, Changsha, Hunan 410083, China
[b] Chemical Engineering Department, New Mexico State University, Las Cruces, NM 88003, USA
[c] Key Laboratory of Resources Chemistry of Nonferrous Metals (Ministry of Education), Changsha 410083, China

HIGHLIGHTS

- Elucidation of chemical adsorption of 2-naphthol on the TEPA polymeric adsorbent.
- Detailed studies on adsorption equilibrium and kinetics of 2-naphthol.
- Correlation of adsorption kinetic data with two models.
- Repeated adsorption breakthrough curves and correlation with several dynamic models.
- Good agreement between the equilibrium and kinetic capacity.

GRAPHICAL ABSTRACT

Repeated adsorption breakthrough curves of 2-naphthol from a TEPA-3 column.

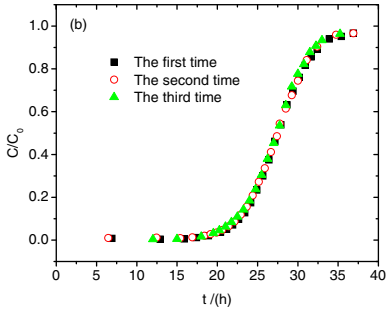

ARTICLE INFO

Article history:
Received 22 October 2012
Received in revised form 7 December 2012
Accepted 8 December 2012
Available online 14 December 2012

Keywords:
Adsorption
Thermodynamics
Kinetics
Breakthrough
2-Naphthol

ABSTRACT

Adsorptive removal of 2-naphthol from aqueous solutions by a hypercrosslinked poly(styrene-co-divinylbenzene) (PS) resin (TEPA-3) was investigated under adsorption equilibrium, kinetic and column breakthrough conditions. The adsorption of 2-naphthol in aqueous solutions on resin TEPA-3 is very effective as indicated by the high adsorption equilibrium capacity (210.0 mg/g at 2-naphthol concentration of 100 mg/L and 298 K). This adsorption process is endothermic because the adsorption capacity increases with the feed solution temperature. The adsorption of 2-naphthol in aqueous solutions on resin TEPA-3 could reach equilibrium within 180 min, the adsorption kinetic data can be well correlated by the pseudo-second-order rate equation and a micropore diffusion model, and the diffusion activation energy was determined to be 4.998 kJ/mol. The dynamic adsorption capacities obtained in the column breakthrough experiments are within 90% of the corresponding equilibrium capacities obtained in the batch experiments. The Bed Depth Service Time model, the Thomas and Yoon model are suitable for fitting the column breakthrough data. The used TEPA-3 resin saturated with 2-naphthol can be effectively regenerated with a mixture of 1% of sodium hydroxide (w/v) and 50% of ethanol aqueous solution (v/v).

1. Introduction

A hypercrosslinked poly(styrene-co-divinylbenzene) (PS) resin (TEPA-3) was successfully prepared from a macroporous crosslinked chloromethylated PS by a self Friedel–Crafts alkylation reaction followed with a nucleophilic substitution reaction with

* Corresponding authors. Address: School of Chemistry and Chemical Engineering, Central South University, Changsha, Hunan 410083, China. Tel./fax: +86 731 88879616 (J. Huang), tel.: +1 575 6464346; fax: +1 575 6467706 (S. Deng).
E-mail addresses: jianhanhuang@csu.edu.cn (J. Huang), sdeng@nmsu.edu (S. Deng).

1385-8947/$ - see front matter © 2012 Elsevier B.V. All rights reserved.
http://dx.doi.org/10.1016/j.cej.2012.12.032

tetraethylenepentamine [1]. The pore textural properties of TEPA showed that micropore Brunauer–Emmett–Teller (BET) surface area and micropore volume are more than one-half of the total surface area and pore volume, suggesting its potential capability of separating organic compounds with smaller molecular size like 2-naphthol from the others with a more bulky molecular size like berberine hydrochloride from aqueous solutions. Actually, the dynamic separation experiment demonstrated that TEPA-3 separated 2-naphthol from berberine hydrochloride effectively and the purity of berberine hydrochloride in the aqueous solution increased from 66.7% to 99.4% (w/w). On the other hand, the adsorption of 2-naphthol in aqueous solution on resin TEPA-3 was shown to be very efficient as indicated by the high equilibrium adsorption capacity (210.0 mg/g at 2-naphthol concentration of 100 mg/L and 298 K). This capacity is much larger than that of many adsorbents including the commercial XAD-4 and XAD-7 resins [2] as well as the hydroquinone modified hypercrosslinked PS resin and carbons [3,4]. It is possible to employ resin TEPA-3 as a specific polymeric adsorbent for the adsorptive removal of 2-naphthol and its derivatives from aqueous solutions. For this reason, the adsorption behaviors of 2-naphthol in aqueous solutions on resin TEPA-3 were discussed in detail in the present study and the potential application of TEPA-3 for the adsorptive removal of 2-naphthol from wastewater was also described.

2-Naphthol ($C_{10}H_7OH$) and its derivatives are typical organic pollutants in wastewater of many chemical plants. Treatment of wastewater containing 2-naphthol is a very urgent problem for environmental protection for every country, which is studied by various methods such as precipitation, microbial degradation, oxidation, extraction with solvents and adsorption [3–14]. Adsorption based on adsorbents is shown to be effective among these methods due to the large adsorption capacity, relatively high selectivity, structural diversity and easy regenerations for repeated use [4,7,9]. Amberlite XAD-4 is considered as one of the best commercial polymeric adsorbents of the second-generation PS copolymers for removing organic pollutants from aqueous solutions [15,16]. Many experimental studies have stated that XAD-4 is a very effective polymeric adsorbent for adsorption of non-polar or weakly polar aromatic compounds from an aqueous solution [17–20]. Recently, the hypercrosslinked PS resins are considered as one kind of super polymeric adsorbents for adsorptive removal of aromatic compounds from aqueous solution due to their relatively high BET surface area and unique pore structure [21,22]. In addition, the hypercrosslinked PS resins can also be employed as the column packing materials in high-performance liquid chromatography (HPLC), ion size-exclusion chromatography materials and solid-phase extraction materials for gases, organic contaminants and organic vapors. The hypercrosslinked PS resins is carried out from a linear PS or a low cross-linked PS by adding bifunctional (or polyfunctional) crosslinking reagents in a thermodynamically good solvent. Firstly, the crosslinking agent reacts with one of its active sites with a phenyl ring of a polymeric chain, thus forming a crosslinking bridge with an unsubstituted phenyl ring in the same (different) chain, and then favorable, strongly expanded conformations of the solvated PS chains are fixed and preserved, leading to a major shift of their pore diameter distribution from predominately mesopores to micropores distribution, and hence resulting in a sharp increase of the BET surface area and pore volume. In particular, surface chemical modification of the hypercrosslinked PS resins by introduction of some specific functional groups like amino groups on the surface of the hypercrosslinked PS resins makes them even more effective [23–25].

In this study, we applied a tetraethylenepentamine-modified hypercrosslinked PS resin TEPA-3 as a specific polymeric adsorbent for the adsorption of 2-naphthol from aqueous solutions. The adsorption equilibrium, kinetics and column breakthrough of 2-naphthol on resin TEPA-3 were measured and analyzed in detail.

2. Experimental

2.1. Adsorption isotherms

Preparation, characterization and pore textural properties of the polymeric adsorbent (resin TEPA-3) studied in this work were described in our previous work [1]. For the equilibrium experiment, about 0.1000 g of resin TEPA-3 sample were mixed with 50 mL of a series of 2-naphthol aqueous solutions with concentrations of about 200, 400, 600, 800 and 1000 mg/L. The series of solutions were then shaken in a thermostatic oscillator at a desired temperature (298, 313 or 328 K) and an agitation speed of 220 rpm until the equilibrium was reached. To determine the equilibrium concentration of 2-naphthol in an aqueous solution, a working curve of UV absorbency-concentration was firstly developed. The absorbency of a standard 2-naphthol aqueous solution with different known concentrations was analyzed by a Lambda 35 UV–VIS spectrometer (Perkin Elmer) at the wavelength of 273.7 nm. A well-fitted regression equation, $A = 0.03064C - 0.03036$, was obtained with a correlation coefficient R^2 of 0.9999. Then the absorbency of the 2-naphthol solution adsorbed by the resin was measured and the equilibrium concentration of 2-naphthol C_e (mg/L) was calculated based on the working curve. The equilibrium adsorption capacity q_e (mg/g) was determined based on the following equation:

$$q_e = (C_0 - C_e) \cdot V/W \quad (1)$$

where C_0 is the initial concentration of 2-naphthol (mg/L), V is the volume of the solution (L) and W is the mass of the resin (g).

2.2. Adsorption kinetics

For the kinetic experiments, about 1.0000 g of the resin was mixed with 250 mL of a 2-naphthol solution with an initial concentration of 519.9 mg/L. The flask was then continuously shaken at a desired temperature (298, 313 or 328 K) until adsorption equilibrium was reached. In this process, 0.5 mL of the solution was withdrawn at a 10-min interval in the first hour and a 30-min interval in the subsequent hour and the concentration of 2-naphthol was determined, the adsorption capacity at a contact time t was calculated as:

$$q_t = (C_0 - C_t) \cdot V/W \quad (2)$$

where q_t (mg/g) and C_t are the adsorption capacity and the concentration at contact time t (mg/L), respectively.

2.3. Column adsorption and desorption breakthrough

For the column adsorption and desorption breakthrough experiment, 7.120 g of resin TEPA-3 was firstly immersed in de-ionized water at 298 K for about 24 h (the wetted resin was measured to be 17.0 mL) and then densely packed in a glass column with an inner diameter of 19 mm (D = 19 mm). The 2-naphthol aqueous solution with a certain initial concentration (C_0 = 320.2, 507.7 or 805.7 mg/L) was passed through the resin column at a certain flow rate (Q = 3.1, 6.2 or 9.3 mL/min) and the concentration of 2-naphthol in the effluent from the column exit, C (mg/L), was continuously recorded until it reached the initial concentration. After the adsorption breakthrough run, the resin column was rinsed with 10 mL of de-ionized water and a certain desorption solvent was applied to the desorption process and the concentration of 2-naphthol was determined until it was zero.

3. Results and discussion

3.1. Adsorption comparisons

By changing the Friedel–Crafts reaction time as 0.5, 1, 3, 5 and 9 h, respectively, five kinds of tetraethylenepentamine-modified hypercrosslinked PS resins labeled TEPA-0.5, TEPA-1, TEPA-3, TEPA-5 and TEPA-8 were prepared in this study and their characteristic parameters are shown in Table S1. Due to the different Friedel–Crafts reaction time, the residual chlorine content of the intermediate products after the Friedel–Crafts reaction should be different and a longer Friedel–Crafts reaction time results in lower residual chlorine content. In particular, the residual chlorine content of the intermediate product will determine its pore structure and the intermediate product with lower residual chlorine content should have a higher BET surface area and pore volume. Additionally, after the nucleophilic substitution reaction of the intermediate products with tetraethylenepentamine, some of the residual chlorine will be substituted by the functional groups (–NH–/NH_2) and the intermediate products with higher residual chlorine content will upload more –NH–/NH_2 groups, inducing a higher polarity. In conclusion, sample TEPA-0.5 should possess the lowest BET surface area and pore structure while the highest uploading amount of the –NH–/NH_2 groups on the surface, sample TEPA-8 should possesses the highest BET surface area and pore volume while the lowest uploading amount of –NH–/NH_2 groups on the surface, suggesting their different adsorption selectivity for a specific aromatic compound from aqueous solutions. As compared the equilibrium adsorption capacities of 2-naphthol on these series of adsorbents at the same initial concentration of 511.7 mg/L and 298 K (see Fig. S1), TEPA-3 has the largest equilibrium capacity among these five adsorbents. The BET specific surface area of the adsorbent, pore structure of the adsorbent, and the matching of the pore size of the adsorbent with the size of the adsorbate as well as the polarity matching between the adsorbent and the adsorbate are the main factors influencing the adsorption. The BET surface area of TEPA-3 is much higher than that of TEPA-0.5 (difference: 128 m^2/g) and weak basic exchange capacity of TEPA-3 is much higher than that of TEPA-8 (difference 0.242 mmol/g), the uploaded functional groups (–NH–/NH_2) can result in an acid-base neutralization between 2-naphthol and TEPA resin, which is related to chemical adsorption. So it is entirely possible that the combinations of the appropriate pore structure and the appropriate uploading amount of the functional groups make TEPA-3 a better adsorbent for 2-naphthol.

To account for the necessity of the nucleophilic substitution reaction of HJ-33 (a) (the intermediate product obtained by the Friedel–Crafts reaction of macroporous crosslinked chloromethylated poly(styrene-co-divinylbenzene) under the catalysis of $FeCl_3$ with the reaction time of 3 h) with tetraethylenepentamine, the adsorption isotherms of 2-naphthol on TEPA-3 and HJ-33 (a) were measured firstly at 298 K and the results are shown in Fig. 1. The equilibrium adsorption capacity of 2-naphthol on TEPA-3 is obviously larger than that on HJ-33 (a) at the same equilibrium concentration. There is an obvious decrease of the BET surface area and pore volume after the nucleophilic substitution reaction (the BET surface area and pore volume of HJ-33 (a) were 938.5 m^2/g and 0.6755 cm^3/g, respectively), while the uploaded functional –NH–/NH_2 on the surface of TEPA-3 may enhance the adsorption due to the polarity matching [26–28].

The functional groups on a macroporous polymeric adsorbent are very important for separation and purification of some specific organic compounds from aqueous/non-aqueous solution and these functional groups are frequently regarded as a solid-phase extraction (SPE) reagent [29,30]. Here we plotted the increased adsorption capacity of 2-naphthol on TEPA-3 in contrast with HJ-33 (a) (q_a, where $q_a = q_{e(\text{TEPA-3})} - qe(\text{HJ-33(a)})$) on dependency of the equilibrium concentration of 2-naphthol. It is interesting to see that plotting of q_a versus C_e does not present a linear relationship (see Fig. S2) while a complete linear relationship is appeared for the plotting of log q_a versus log C_e by using a Freundlich isotherm equation as $\log q_e = (1/n)\log C_e + \log K_F$.

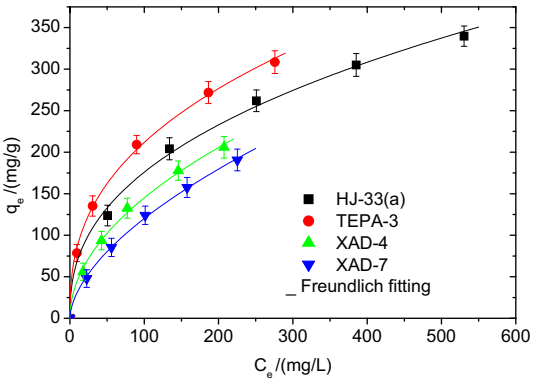

Fig. 1. Isotherms of 2-naphthol adsorption on HJ-33 (a), TEPA-3, XAD-4 and XAD-7 from aqueous solution with the temperature at 298 K.

Some commercial adsorbents such as XAD-4 and XAD-7 are considered the most efficient polymeric adsorbents for adsorptive removal of aromatic pollutants from wastewater. The isotherm of 2-naphthol on TEPA-3 is then compared with those on XAD-4 and XAD-7 at 298 K (see Fig. 1). It is found that the adsorption capacity of 2-naphthol on TEPA-3 is much larger than that on XAD-4 and XAD-7. At an equilibrium concentration of 100 mg/L, the 2-naphthol adsorption capacity on TEPA-3, XAD-4 and XAD-7 are shown to be 210.0, 144.6 and 99.23 mg/g, respectively. In addition, when we compared the adsorption of 2-naphthol on TEPA-3 with that on graphene and graphene oxide [2] and activated carbon [9], TEPA-3 is shown to be as efficient as the activated carbon for the adsorptive removal of 2-naphthol from aqueous solutions. Some low-cost materials or even wastes such as alumina [7], marine sediments [12], laponite [13] seem economically attractive for practical application of 2-naphthol from aqueous solution. However, these materials are inferior to TEPA-3 for adsorption of 2-naphthol. In addition, when we compared the adsorption of 2-naphthol on TEPA-3 with some other polymeric adsorbents reported in the literatures [3,4,14], TEAP-3 is also proven superior to some nonionic polymeric resins and hypercrosslinked resins.

3.2. Effect of the adsorbent dose on the adsorption

The effect of the adsorbent dose on the removal percentage of 2-napthol as well as the equilibrium adsorption capacity of 2-napthol on TEPA-3 is illustrated in Fig. S3. With the initial concentration of 2-naphthol at 511.7 mg/L, the removal efficiency of 2-napthol from aqueous solutions increases rapidly from 17.86% to 93.23% with the adsorbent dose from 0.0406 to 0.3103 g/100 mL aqueous solution and thereafter marginally increases, which demonstrates that TEPA-3 is an excellent adsorbent for adsorptive removal of 2-napthol from aqueous solutions.

3.3. Effect of solution pH on the adsorption

Fig. 2 indicates that the adsorption of 2-naphthol on TEPA-3 is very sensitive to the solution pH. The adsorption capacity of 2-naphthol is nearly invariable (about 200 mg/g) at pH = 3.74–7.78

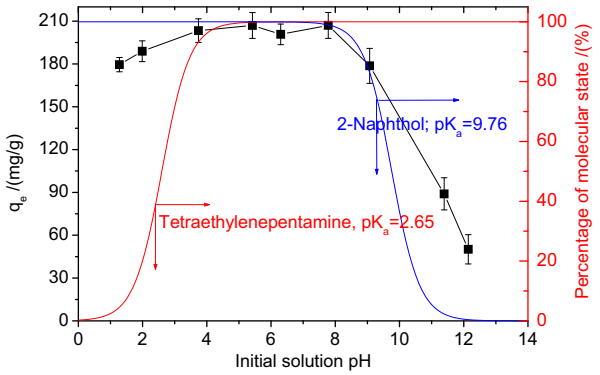

Fig. 2. Adsorption capacity of 2-naphthol on TEPA-3 from aqueous solution on dependency of the solution pH.

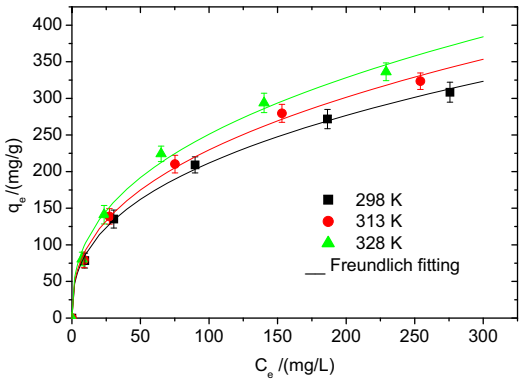

Fig. 3. Isotherms of 2-naphthol adsorption on TEPA-3 from aqueous solution with the temperature at 298, 313 and 328 K, respectively.

and is slightly decreased at pH < 3.74 while is a much decreased at pH > 7.78 and it is reduced to about 50 mg/g at pH = 12.14.

According to the reported pK_a of 2-naphthol (pK_a = 9.76) in aqueous solution [31], the dissociation curve of 2-naphthol in aqueous solution were predicted as a function of the solution pH and shown in Fig. 2. As pH = 3.74–12.14, the 2-naphthol adsorption on TEPA-3 has the same trend as the dissociation curve of 2-naphthol in aqueous solution, which displays that the molecular state of 2-naphthol is suitable for the adsorption while the ionic state is not suitable (there maybe exist competition adsorption between the OH^- and 2-naphthol ions on the resin active sites at a higher pH solution). As pH < 3.74, the ionization equilibrium of 2-naphthol will be affected due to the superfluous protons in aqueous solution and more 2-naphthol molecules will be obtained, which should enable a larger adsorption capacity on TEPA-3 if the functional –NH–/NH_2 groups on the surface of TEPA-3 do not considered in this study. Obviously, the deduction is opposite to the observation in Fig. 2. Note that there is 0.704 mmol/g of –NH–/NH_2 groups were uploaded on the surface of TEPA-3 and these amino groups should have an effect on the adsorption. The pK_a of tetraethylenepentamine is determined to be 2.65 [32] and hence the dissociation curve of tetraethylenepentamine in aqueous solution were also predicted as a function of the solution pH and also displayed in Fig. 2. As pH < 3.74, more 2-naphthol molecules are obtained while the –NH–/NH_2 groups of tetraethylenepentamine uploaded on the surface of TEPA-3 are gradually protonized, which is disadvantageous for the adsorption. From the above results, we can make a conclusion that there should be a few –NH–/NH_2 groups are uploaded on the surface of TEPA-3 and 2-naphthol molecules cannot be completely desorbed by 0.01 mol/L of sodium hydroxide aqueous solution.

3.4. Effect of inorganic salts on the adsorption

Owing to the coexistence of inorganic salts such as sodium sulfite (Na_2SO_3), sodium sulfate (Na_2SO_4) and sodium chloride (NaCl) with the industrial wastewater containing 2-naphthol at a comparatively high level, the effect of Na_2SO_3, Na_2SO_4 and NaCl on the ability of TEPA-3 to remove 2-naphthol from aqueous solution is determined, and the results are depicted in Fig. S4. It is shown that the percentage of Na_2SO_3, Na_2SO_4 and NaCl almost exhibits no effect on the adsorption of 2-naphthol on TEPA-3 at 298 K.

3.5. Adsorption isotherms and thermodynamics

Fig. 3 displays the adsorption isotherms of 2-naphthol onto TEPA-3 in aqueous solution at 298, 313 and 328 K, respectively. It is interesting to observe that the adsorption capacity increases with increasing the feed temperature [33,34], implying an endothermic adsorption process and a different phenomenon from XAD-4. The Langmuir and Freundlich isotherm equations were used to correlate the adsorption isotherms plotted in Fig. 3 [35,36], and the fitted parameters q_m, K_L, K_F and n as well as the correlation coefficient (R^2) summarized in Table S2 reveal that both of Langmuir and Freundlich isotherm equations are suitable for fitting the isotherm data due to a high R^2 (>0.98) and the Freundlich equation is more suitable for representing the equilibrium data (R^2 > 0.99). Adsorption enthalpy (ΔH, kJ/mo1) on dependency of the fractional adsorption loading (θ, $\theta = q/q_e$, where q is the considered equilibrium adsorption capacity), adsorption free energy (ΔG, kJ/mo1) and adsorption entropy (ΔS, [J/(mol K)]) was calculated according to the method in ref [37–39] and listed in Table 1. It is obvious that the ΔH are positive, suggesting that 2-naphthol adsorption on TEPA-3 is endothermic and the adsorption is not a simple physical adsorption process while it may involve a weakly chemical bond formation [40]. Meanwhile, the ΔH decreases strongly with increasing of the θ value, which implies that the surface of TEPA-3 is energetic heterogeneous [41–43] and the surface energetic heterogeneity of TEPA-3 can be attributed to the polar interaction between the functional –NH–/NH_2 groups on TEPA-3 and the hydroxyl groups of 2-naphthol. The negative ΔG reveals the adsorption is spontaneous and a higher adsorption temperature gives a more spontaneous process. In particular, the ΔS are positive, which implies a "solvent replacement" is taken place in the process [44,45]. The solvent replacement can be explained as follows. 2-Naphthol can be dissolved in water and it will interact with many water molecules in aqueous solution. TEPA-3 is hydrophilic and it can be used directly in aqueous solution due to introduction of the hydrophilic –NH–/NH_2 groups on the surface and many water molecules surrounded their surfaces as TEPA-3 was fed in aqueous solution. Before 2-naphthol was adsorbed on the surface of TEPA-3, the existing bond between 2-naphthol molecules and water molecules as well as that between TEPA-3 and water molecules had to be broken and then 2-naphthol molecules will take the place of the water molecules and form a possible bond with TEPA-3. This process is called "solvent replacement" [41,42]. Due to the much bulky molecular size of 2-naphthol molecules as compared with the water molecules, the number of water molecules pushed out from the surface on TEPA-3 in the adsorption should be much more abundant than that of 2-naphthol molecules adsorbed on the surface on TEPA-3, leading an increase of the ΔS.

To explain the possible chemical bond formation mechanism between 2-naphthol and TEPA-3 in the present study, the isotherm cycles were performed for a series of 2-naphthol aqueous solution containing TEPA-3 by transforming the temperature of the series of test 2-naphthol solution between 298 K and 328 K (or between

Table 1
Adsorption enthalpies (ΔH), adsorption free energies (ΔG) and adsorption entropies (ΔS) for the 2-naphthol adsorption on TEPA-3 from aqueous solution.

$\theta = q/q_e$	ΔH (kJ/mol)	ΔG (kJ/mol)			ΔS (J/(mol K))		
		298 K	313 K	328 K	298 K	313 K	328 K
0.02850	36.14	−6.112	−6.214	−6.479	141.8	135.3	129.9
0.05700	31.37	−6.112	−6.214	−6.479	125.8	120.1	115.4
0.1140	26.59	−6.112	−6.214	−6.479	109.7	104.8	100.8
0.2280	21.82	−6.112	−6.214	−6.479	93.73	89.57	86.28
0.2850	20.28	−6.112	−6.214	−6.479	88.56	84.65	81.58
0.3135	19.63	−6.112	−6.214	−6.479	86.38	82.57	79.60
0.3705	18.48	−6.112	−6.214	−6.479	82.52	78.90	76.10
0.4275	17.49	−6.112	−6.214	−6.479	79.20	75.73	73.08
0.4845	16.63	−6.112	−6.214	−6.479	76.32	72.98	70.46
0.5130	16.24	−6.112	−6.214	−6.479	75.01	71.74	69.27
0.5984	15.17	−6.112	−6.214	−6.479	71.42	68.32	66.00
0.6270	14.85	−6.112	−6.214	−6.479	70.34	67.30	65.03
0.6555	14.55	−6.112	−6.214	−6.479	69.34	66.34	64.11
0.7125	13.97	−6.112	−6.214	−6.479	67.39	64.49	62.35
0.7695	13.44	−6.112	−6.214	−6.479	65.61	62.79	60.73
0.8265	13.02	−6.112	−6.214	−6.479	64.20	61.45	59.45
0.8549	12.72	−6.112	−6.214	−6.479	63.20	60.49	58.53

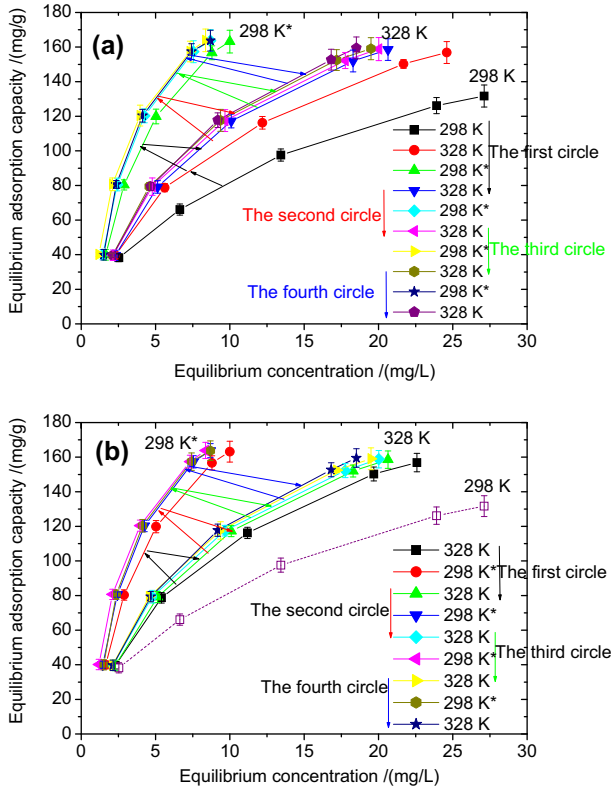

Fig. 4. Isotherm circles for 2-naphthol adsorption on TEPA-3 from aqueous solution between the temperature of 298 K and 328 K (a) as well as that between the temperature of 328 K and 298 K (b).

328 K and 298 K), and 5 h were given at any temperature for the adsorption to reach equilibrium. As can be seen from Fig. 4a, if 298 K was set as the initial temperature for the adsorption and the isotherm of 2-naphthol on TEPA-3 at 298 K is strictly identical to that in Fig. 3 at 298 K. As the temperature increases from 298 K to 328 K and the adsorption at 318 K is enhanced in contrast with that at 298 K, which is accordant with the results in Fig. 3. However, as the temperature is further decreased from 328 K to 298 K (to differentiate the initial temperature 298 K from this temperature, we use 298 K* to represent this new condition), it is surprised to observe that the adsorption is still strengthened and the adsorption at 298 K* is much greater than that at the original 298 K. On the other hand, if 328 K was set as the initial temperature for the adsorption (see Fig. 4b) and the isotherm of 2-naphthol on TEPA-3 at 328 K has no difference from that in Fig. 3 at 328 K. However, as the temperature is then decreased from 328 K to 298 K*, the adsorption cannot return to the position at the initial 298 K while it is much enhanced and the adsorption at 298 K* are much greater than that at 298 K. All of these phenomena are much different from those of XAD-4 (see Fig. S5). The physical adsorption is the dominant mechanism for the adsorption of organic compounds on XAD-4 from aqueous solution and the different isotherm cycle mean that there is a weakly chemical bond formation for the adsorption of 2-naphthol on TEPA-3.

3.6. Adsorption kinetics

Fig. 5 displays the kinetic curves of 2-naphthol adsorption on TEPA-3 from aqueous solution at 298, 313 and 328 K, respectively. The adsorption was very fast in the first hour (the adsorption capacity in the first 1 h is up to 89–94% relative to the equilibrium adsorption capacity) and then slower and at last reaches equilibrium within 180 min, implying that TEPA-3 displays an excellent kinetic property for 2-naphthol. In addition, the required time for the equilibrium is gradually shorter with increasing temperature (about 180 min at 298 K, 150 min at 313 K, and about 120 min at 328 K, respectively), suggesting that a higher temperature induces a faster diffusion rate. The pseudo-second-order equation proposed by Ho and McKay [46,47] was used to analyze the kinetic data:

$$t/q_t = 1/(k_2 \cdot q_e^2) + t/q_e \quad (3)$$

where k_2 is the pseudo-second-order rate constant (g/(mg·min)).

Table S3 summarizes the corresponding model parameters and the very high R^2 (>0.999) suggests that the adsorption kinetic data fitted by the pseudo-second-order rate equation is suitable. Moreover, the calculated equilibrium adsorption capacities ($q_{e,Cal}$) are very close to the experimental ones ($q_{e,Exp}$) at any temperature, further confirming the feasibility of the pseudo-second-order rate equation for the kinetic curves.

There exist a large number of micropores in TEPA-3 and the microporous region was the concentrating distribution for the pore of TEPA-3 and hence a micropore diffusion model was applied in the present study to further analyze the kinetic data [48]. For the fractional adsorption uptake (q_t/q_e) less than 85%, the adsorption kinetics in a microporous adsorbent can be demonstrated as:

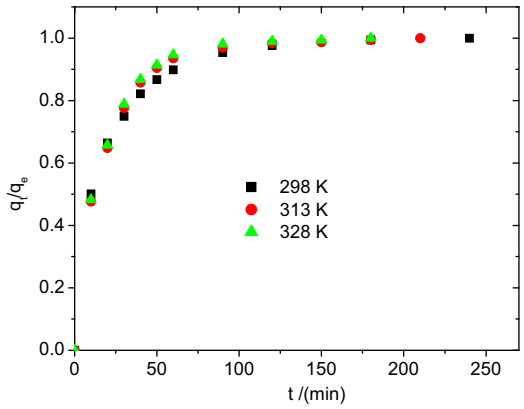

Fig. 5. Kinetic curves of 2-naphthol adsorption on TEPA-3 from aqueous solution with the temperature at 298, 313 and 328 K, respectively.

$$\frac{q_t}{q_e} = \frac{6}{\sqrt{\pi}}\sqrt{\frac{D_c t}{r_c^2}} - \frac{3D_c t}{r_c^2} \tag{4}$$

where D_c is the micropore diffusivity (cm^2/s) and r_c is the crystal diameter of the adsorbent (cm). The adsorption kinetic data shown were fitted to this micropore diffusion model through a nonlinear regression (the correlated parameters according to the micropore diffusion model were shown in Table S4) and the diffusion activation energy E_a of 4.998 kJ/mol was estimated by plotting $\ln(D_c/r_c^2)$ versus $1/T$ (see Fig. S6).

3.7. Adsorption and desorption column breakthrough dynamics

Fig. 6 is the adsorption breakthrough profiles for the dynamic adsorption of 2-naphthol on TEPA-3 packed column from aqueous solution at 298 K. The flow rate of 2-naphthol aqueous solution through the resin column (Q) was varied between 3.1, 6.2 and 9.3 mL/min while the initial concentration of 2-naphthol was altered between 320.2, 507.7 and 805.7 mg/L, respectively. In this study, we defined $C/C_0 = 0.05$ as the breakthrough point and the time required to reach this point was defined as t_b (h). Fig. 6 indicated that the respective t_b was measured to be 32.1, 21.1 and 14.0 h with the initial concentration of 2-naphthol at 320.2, 507.7 and 805.7 mg/L at a constant flow rate (3.1 mL/min) and a higher initial concentration results in a smaller t_b. Additionally, t_b was measured to be 21.1, 9.06 and 5.04 h with a flow rate at 3.1, 6.2 and 9.3 mL/min at a given initial concentration (507.7 mg/L), and a relatively smaller flow rate induces a larger t_b, and therefore a greater V_b (volume of 2-naphthol aqueous solution treated by TEPA-3 at the breakthrough point, and $V_b = Q \cdot t$) due to an increase of the empty bed contact time (EBCT, and EBCT = V_c/Q, where V_c is the volume of the adsorbent in the bed, in this study V_c = 17 mL).

Several adsorption dynamic models are available for describing the adsorption breakthrough in adsorbent columns. The Bed Depth Service Time (BDST), Thomas, Clark and Yoon models given below are applied to analyze the adsorption breakthrough data in this study [49–53].

BDST model:

$$\frac{C}{C_0} = \frac{1}{1 + \exp(\ln(\exp(kN_0Z/U) - 1) - kC_0t)} \tag{5}$$

Thomas model:

$$\frac{C}{C_0} = \frac{1}{1 + \exp[k_T(q_0m_C/Q - C_0t)]} \tag{6}$$

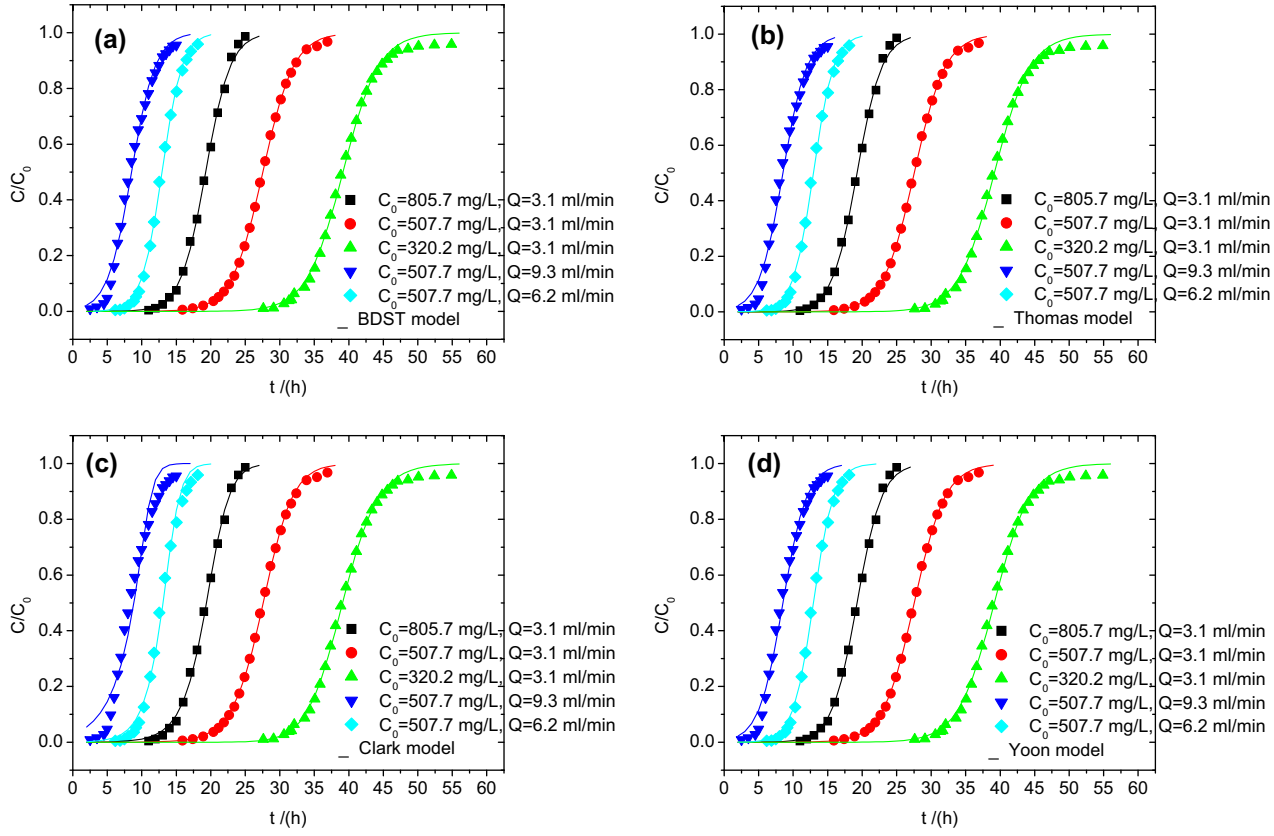

Fig. 6. Breakthrough curves for 2-naphthol adsorption on TEPA-3 packed column with the temperature at 298 K.

Table 2
Recovery efficiency of different solvents for the desorption of 2-naphthol from TEPA-3 resin column.

Solvent	H_2O	1% NaOH (w/v)	5% NaOH (w/v)	20% EtOH (v/v)	50% EtOH (v/v)	95% EtOH (v/v)	1% NaOH (w/v)+20% EtOH (v/v)	1% NaOH (w/v)+50% EtOH (v/v)	5% NaOH (w/v)+20% EtOH (v/v)
Recovery ratio (%)	5.790	75.44	73.70	32.04	93.60	99.12	93.59	99.97	95.78

Clark model:

$$\frac{C}{C_0} = \left(\frac{1}{1 + Ae^{-rt}}\right)^{1/n-1} \quad (7)$$

Yoon model:

$$\frac{C}{C_0} = \frac{\exp(k_{YN}t - k_{YN}t_{0.5})}{1 + \exp(k_{YN}t - k_{YN}t_{0.5})} \quad (8)$$

where C is the concentration of 2-naphthol from the effluent (mg/L). In the BDST model, k is the BDST rate constant [L/(min·mg)], Z is the bed length of the resin column (cm, Z = 6.0 cm in this study), N_0 is the adsorption capacity of the adsorbent bed (mg/mL wet resin) and U is the linear flow velocity of the feed to the bed (cm/min). In the Thomas model, k_T is the Thomas rate constant [L/(min·mg)], q_0 is the maximum adsorption capacity (mg/g), m_C is the weight of the adsorbent in the column (g, m_C = 7.120 g in this study) and Q is the volumetric flow rate (mL/min). In the Clark model, n is the Freundlich constant, A and r are the Clark constants related to the breakthrough point. In the Yoon model, k_{YN} is the Yoon rate constant (min^{-1}) and $t_{0.5}$ is the required time to reach C/C_0 = 0.50.

The four models were used to fit the dynamic curves by a nonlinear regression and the fitted curves were presented in Fig. 6a–d, respectively. Table S5 summarizes the corresponding characteristic parameters. It is interesting to find that the four dynamic models are suitable for characterizing the dynamic data at Q = 3.1 mL/min because of a lesser sum of squares due to error (SSE). At Q = 6.2 mL/min, Clark model is not suitable for fitting the dynamic data and all of these four models are not suitable at Q = 9.3 mL/min. In addition, BDST, Thomas and Yoon models are more suitable for fitting the dynamic data than the Clark model. Table S5 shows that the rate constant k predicted by the BDST model is identical to corresponding k_T by the Thomas model and k_{YN} by the Yoon model, N_0 calculated from the BDST model is also very close to the corresponding q_0 by the Thomas model if the unit can be united, and they are very close to the corresponding experimental dynamic adsorption capacities in Table S5, and both of them are within 90% of the corresponding equilibrium adsorption capacities in the above isotherm section. The $t_{0.5}$ calculated by the Yoon model is very close to the experimental data, which further states that the BDST, Thomas and Yoon models characterize the dynamic data perfectly.

After the dynamic adsorption breakthrough experiments, the TEPA-3 resin column was gently rinsed with 10 mL of de-ionized water and then different solvents were employed for the desorption process. The recovery efficiency of different solvents for desorbing 2-naphthol from the resin column was listed in Table 2. It is clear that water can hardly desorb 2-naphthol from the resin column and only 5.79% of 2-naphthol is desorbed from the resin. However, sodium hydroxide aqueous solution (NaOH) can only partly desorb 2-naphthol from the resin column and 73.7% of 2-naphthol can be recovered as 5% of NaOH (w/v) is applied. Meanwhile, Ethanol aqueous solution (EtOH) can practically desorb 2-naphthol from the resin column and increase of concentration of EtOH can improve the recovery efficiency and recovery efficiency of 99.12% is achieved as 95% of EtOH (v/v) is used. In particular, a mixture of NaOH and EtOH can greatly improve the recovery efficiency and the recovery efficiency of 99.97% is achieved as a mixture of 1% of NaOH (w/v) and 50% of EtOH (v/v) was employed as the desorption solvent and we used this mixture as the regenerant in the dynamic desorption process. For the resin column with the initial concentration of 507.7 mg/L and a flow rate of 3.1 mL/min, 200 mL 1% of NaOH (w/v) and 50% of EtOH (v/v) was passed through the resin column, only 14.0 bed volumes of the desorption solvent was needed to completely regenerate the resin column and the dynamic desorption amount of 2-naphthol was determined to be 2470 mg (see Fig. 7a), which is excellently coincident with the dynamic adsorption amounts (2491 mg). We also did the second and third adsorption breakthrough run after the regeneration, as can be seen from Fig. 7b and the second and third breakthrough run is almost identical to the first one.

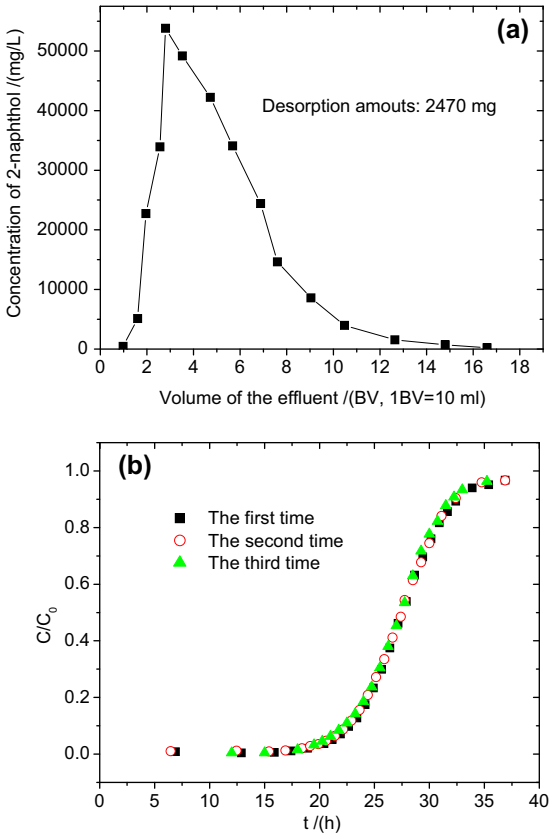

Fig. 7. (a) Dynamic desorption of 2-naphthol from TEPA-3 column using a mixture of 1% of sodium hydroxide and 50% of ethanol aqueous solution and (b) the first, second and third dynamic adsorption curves of 2-naphthol on TEPA-3.

4. Conclusions

The adsorption of 2-naphthol on resin TEPA-3 from aqueous solutions was effective, and the adsorption capacity increased with increasing temperature. The adsorption enthalpies are positive, suggesting the adsorption is an endothermic process, and the adsorption was not a simple physical adsorption process that may involves a weak chemical bond formation. The adsorption entropies were also positive, which implied that a "solvent replacement" process is taken place due to the much bigger molec-

ular size of 2-naphthol molecule than the water molecule. The adsorption of 2-naphthol on TEPA-3 is sensitive to the solution pH, the adsorption capacity 2-naphthol is almost invariable at the solution pH of 3.74–7.78, it is slightly decreased at a solution pH below 3.74 while there is a much great decrease at a solution pH higher than 7.78. The kinetic adsorption results indicated that the adsorption reaches an equilibrium with 180 min and the kinetic data could well be fitted by the pseudo-second-order rate equation and the micropore diffusion model. The column adsorption dynamic results showed that the dynamic adsorption capacities of 2-naphthol on TEPA-3 were predicted to be 311.2, 349.9, 396.5 mg/g at the initial concentration of 320.2, 507.7 and 805.7 mg/L, respectively, which are within 90% of the corresponding equilibrium adsorption capacities obtained in the batch experiments. The used resin column saturated with 2-naphthol could be effectively regenerated by a mixture of 1% of NaOH (w/v) and 50% of EtOH (v/v), and the resin performance did not change in three cycles.

Acknowledgment

This work was partially supported by the National Natural Science Foundation of China (No. 21174163) and the Shenghua Yuying Project of Central South University.

Appendix A. Supplementary material

Supplementary data associated with this article can be found, in the online version, at http://dx.doi.org/10.1016/j.cej.2012.12.032.

References

[1] Y. Li, R.F. Cao, X.F. Wu, J.H. Huang, S.G. Deng, X.Y. Lu, A hypercrosslinked poly(styrene-co-divinylbenzene) (PS) resin as a specific polymeric adsorbent for purification of berberine hydrochloride from aqueous solutions, submitted for publication.
[2] Z.G. Pei, L.Y. Li, L.X. Sun, S.Z. Zhang, X.Q. Shan, S. Yang, B. Wen, Adsorption characteristics of 1,2,4-trichlorobenzene, 2,4,6-trichlorophenol, 2-naphthol and naphthalene on graphene and graphene oxide, Carbon 51 (2013) 156–163.
[3] J.H. Huang, B. Yuan, X.F. Wu, S.G. Deng, A comparative adsorption study of b-naphthol on four polymeric adsorbents from aqueous solutions, J. Colloid Interf. Sci. 380 (2012) 166–172.
[4] C.L. He, J.H. Huang, C. Yan, J.B. Liu, L.B. Deng, K.L. Huang, Adsorption behaviors of a novel carbonyl and hydroxyl groups modified hyper-cross-linked poly(styrene-co-divinylbenzene) resin for β-naphthol from aqueous solution, J. Hazard. Mater. 180 (2010) 634–639.
[5] S. Qourzal, N. Barka, M. Tamimi, A. Assabbane, Y. Ait-Ichou, Photodegradation of 2-naphthol in water by artificial light illumination using TiO_2 photocatalyst: identification of intermediates and the reaction pathway, Appl. Catal. A 334 (2008) 386–393.
[6] S. Qourzal, M. Tamimi, A. Assabbane, Y. Ait-Ichou, Photocatalytic degradation and adsorption of 2-naphthol on suspended TiO_2 surface in a dynamic reactor, J. Colloid Interf. Sci. 286 (2005) 621–626.
[7] K. Esumi, K. Sakai, K. Torigoe, Reexamination of 2-naphthol adsolubilization on alumina with sodium dodecyl sulfate adsorption, J. Colloid Interf. Sci. 224 (2000) 198–201.
[8] S. Zang, B. Lian, Synergistic degradation of 2-naphthol by Fusarium proliferatum and Bacillus subtilis in wastewater, J. Hazard. Mater. 166 (2009) 33–38.
[9] M. Anbia, S.E. Moradi, Adsorption of naphthalene-derived compounds from water by chemically oxidized nanoporous carbon, Chem. Eng. J. 148 (2009) 452–458.
[10] D. Tsurumi, K. Sakai, T. Yoshimura, K. Esumi, Adsolubilization of 2-naphthol into adsorbed layers of triblock PEO–PPO–PEO copolymers on hydrophobic silica particles, J. Colloid Interf. Sci. 302 (2006) 82–86.
[11] S. Qourzal, N. Barka, M. Tamimi, A. Assabbane, A. Nounah, A. Ihlal, Y. Ait-Ichou, Sol–gel synthesis of TiO_2–SiO_2 photocatalyst for β-naphthol photodegradation, Mater. Sci. Eng. C 29 (2009) 1616–1620.
[12] X.K. Zhao, G.P. Yang, Study on the sorption of 2-naphthol on marine sediments, Colloids Surf. A 211 (2002) 259–266.
[13] K. Esumi, K. Yoshida, K. Torigoe, Y. Koide, Sorption of 2-naphthol and copper ions by cationic surfactant-adsorbed laponite, Colloids Surf. A 160 (1999) 247–250.
[14] Z.Y. Xu, Q.X. Zhang, J.L. Chen, L.S. Wang, G.K. Anderson, Adsorption of naphthalene derivatives on hypercrosslinked polymeric adsorbents, Chemosphere 38 (1999) 2003–2011.
[15] V. Davankov, M. Tsyurupa, M. Ilyin, L. Pavlova, Hypercross-linked polystyrene and its potentials for liquid chromatography: a mini-review, J. Chromatogr. A 965 (2002) 65–73.
[16] M. Sinan Bilgili, Adsorption of 4-chlorophenol from aqueous solutions by xad-4 resin: isotherm, kinetic, and thermodynamic analysis, J. Hazard. Mater. 137 (2006) 157–164.
[17] G.Q. Xiao, L.P. Long, Efficient removal of aniline by a water-compatible microporous and mesoporous hyper-cross-linked resin and XAD-4 resin: a comparative study, Appl. Surf. Sci. 258 (2012) 6465–6471.
[18] A.M. Li, Q.X. Zhang, J.L. Chen, Z.H. Fei, C. Long, W.X. Li, Adsorption of phenolic compounds on Amberlite XAD-4 and its acetylated derivative MX-4, React. Funct. Polym. 49 (2001) 225–233.
[19] L.G.T. dos Reis, N.F. Robaina, W.F. Pacheco, R.J. Cassella, Separation of malachite green and methyl green cationic dyes from aqueous medium by adsorption on Amberlite XAD-2 and XAD-4 resins using sodium dodecylsulfate as carrier, Chem. Eng. J. 171 (2011) 532–540.
[20] L.E. Vera-Avila, J.L. Gallegos-Perez, E. Camacho-Frias, Frontal analysis of aqueous phenol solutions in Amberlite XAD-4 columns: implications on the operation and design of solid phase extraction systems, Talanta 50 (1999) 509–526.
[21] G.I. Rosenberg, A.S. Shabaeva, V.S. Moryakov, T.G. Musin, M.P. Tsyurupa, V.A. Davankovsorption, Properties of hypercrosslinked polystyrene sorbents, React. Polym. 1 (1983) 175–182.
[22] M.P. Tsyurupa, V.A. Davankov, Hypercrosslinked polymers: basic principle of preparing the new class of polymeric materials, React. Funct. Polym. 53 (2002) 193–203.
[23] J.H. Huang, X.Y. Jin, J.L. Mao, B. Yuan, R.J. Deng, S.G. Deng, Synthesis, characterization and adsorption properties of diethylenetriamine-modified hypercrosslinked resins for efficient removal of salicylic acid from aqueous solution, J. Hazard. Mater. 217–218 (2012) 406–415.
[24] B.C. Pan, Q.J. Zhang, B.J. Pan, W.M. Zhang, W. Du, H.Q. Ren, Removal of aromatic sulfonates from aqueous media by aminated polymeric sorbents: concentration-dependent selectivity and the application, Microp. Mesop. Mater. 116 (2008) 63–69.
[25] W.M. Zhang, Q. Du, B.C. Pan, L. Lv, C.H. Hong, Z.M. Jiang, D.Y. Kong, Adsorption equilibrium and heat of phenol onto aminated polymeric resins from aqueous solution, Colloids Surf. A 346 (2009) 34–38.
[26] P.N. Breysse, A.M. Cappabianca, T.A. Hall, T. Risby, Effect of polarity on the adsorption of dichlorobenzene isomers, Carbon 25 (1987) 803–808.
[27] J.H. Huang, X.Y. Jin, S.G. Deng, Phenol adsorption on an N-methylacetamide-modified hypercrosslinked resin from aqueous solutions, Chem. Eng. J. 192 (2012) 192–200.
[28] M.A. Abdullah, L. Chiang, M. Nadeem, Comparative evaluation of adsorption kinetics and isotherms of a natural product removal by Amberlite polymeric adsorbents, Chem. Eng. J. 146 (2009) 370–376.
[29] M. Lee, S.Y. Oh, T.S. Pathak, I.R. Paeng, B.Y. Cho, K.J. Paeng, Selective solid-phase extraction of catecholamines by the chemically modified polymeric adsorbents with crown ether, J. Chromatogr. A 1160 (2007) 340–344.
[30] B.C. Pan, X.Q. Chen, B.J. Pan, W.M. Zhang, X. Zhang, Q.X. Zhang, Preparation of an aminated macroreticular resin adsorbent and its adsorption of p-nitrophenol from water, J. Hazard. Mater. 137 (2006) 1236–1240.
[31] J.T. Wang, Q.M. Hu, B.S. Zhang, Y.M. Wang, Organic Chemistry, Nankai University Press, Tianjing, 1998.
[32] C.N. Reilley, J.H. Holloway, The stability of metal-tetraethylenepentamine complexes, J. Am. Chem. Soc. 80 (1958) 2917–2919.
[33] B.L. He, W.Q. Huang, Ion Exchange and Adsorption Resin, Shanghai Science and Technology Education Press, Shanghai, 1995.
[34] D.M. Ruthven, Principles and Adsorption and Adsorption Processes, Willey, New York, 1984.
[35] I. Langmuir, The constitution and fundamental properties of solids and liquids. Part I. Solids, J. Am. Chem. Soc. 38 (1916) 2221–2295.
[36] H.M.F. Freundlich, Über die adsorption in lösungen, Z. Phys. Chem. 57A (1906) 385–470.
[37] J.H. Huang, R.J. Deng, K.L. Huang, Equilibria and kinetics of phenol adsorption on a toluene-modified hyper-cross-linked poly(styrene-co-divinylbenzene) resin, Chem. Eng. J. 171 (2011) 951–957.
[38] H.T. Li, M.C. Xu, Z.Q. Shi, B.L. He, Isotherm analysis of phenol adsorption on polymeric adsorbents from nonaqueous solution, J. Colloid Interf. Sci. 271 (2004) 47–54.
[39] J.G. Cai, A.M. Li, H.Y. Shi, Z.H. Fei, C. Long, Q.X. Zhang, Adsorption characteristics of aniline and 4-methylaniline onto bifunctional polymeric adsorbent modified by sulfonic groups, J. Hazard. Mater. 124 (2005) 173–180.
[40] H.X. Hu, X.M. Wang, S.Y. Li, J.H. Huang, S.G. Deng, Bisphenol-A modified hyper-cross-linked polystyrene resin for salicylic acid removal from aqueous solution: adsorption equilibrium, kinetics and breakthrough studies, J. Colloid Interf. Sci. 372 (2012) 108–112.
[41] H.T. Li, Y.C. Jiao, M.C. Xu, Z.Q. Shi, B.L. He, Thermodynamics aspect of tannin sorption on polymeric adsorbents, Polymer 45 (2004) 181–188.
[42] B. Charmas, R. Leboda, Effect of surface heterogeneity on adsorption on solid surfaces: application of inverse gas chromatography in the studies of energetic heterogeneity of adsorbents, J. Chromatogr. A 886 (2000) 133–152.
[43] M.M. Seredych, V.M. Gun'ko, A. Gierak, Structural and energetic heterogeneities and adsorptive properties of synthetic carbon adsorbents, Appl. Surf. Sci. 242 (2005) 154–161.

[44] J.H. Huang, Treatment of phenol and p-cresol in aqueous solution by adsorption using a carbonylated hypercrosslinked polymeric adsorbent, J. Hazard. Mater. 168 (2009) 1028–1034.
[45] W.M. Zhang, C.H. Hong, B.C. Pan, Q.J. Zhang, P.J. Jiang, K. Jia, Removal enhancement of 1-naphthol and 1-naphthylamine in single and binary aqueous phase by acid–basic interactions with polymer adsorbents, J. Hazard. Mater. 158 (2008) 293–299.
[46] Y.S. Ho, Review of second-order models for adsorption systems, J. Hazard. Mater. 136 (1998) 681–689.
[47] Y.S. Ho, Effect of pH on lead removal from water using tree fern as the sorbent, Bioresource Technol. 96 (2005) 1292–1296.
[48] D.M. Ruthven, S. Farooq, K.S. Knaebel, Pressure Swing Adsorption, VCH, New York, 1994.
[49] G. Bohart, E.Q. Adams, Some aspects of the behavior of charcoal with respect to chlorine, J. Am. Chem. Soc. 42 (1920) 523–544.
[50] H.C. Thomas, Heterogeneous ion exchange in a flowing system, J. Am. Chem. Soc. 66 (1944) 1664–1666.
[51] R.M. Clark, Evaluating the cost and performance of field-scale granular activated carbon systems, Environ. Sci. Technol. 21 (1987) 573–580.
[52] Y.H. Yoon, J.H. Nelson, Application of gas adsorption kinetics. I. A theoretical model for respirator cartridge service time, Am. Indian Hygiene Assoc. J. 45 (1984) 509–516.
[53] V.C. Srivastava, B. Prasad, I.M. Mishra, I.D. Mall, M.M. Swamy, Prediction of breakthrough curves for sorptive removal of phenol by bagasse fly ash packed bed, Ind. Eng. Chem. Res. 47 (2008) 1603–1613.